Biogeosciences
Open Access
Discussions

Quantifying the impact of ocean acidification on our future climate

R. J. Matear[1,2] **and A. Lenton**[1,2]

[1]Centre for Australian Weather and Climate Research (CAWCR) – a partnership between CSIRO and the Bureau of Meteorology, CSIRO Marine and Atmospheric Research, CSIRO Marine Laboratories, GPO Box 1538, Hobart, Tasmania, Australia
[2]CSIRO Marine Research, Hobart, Australia

Correspondence to: R. J. Matear (richard.matear@csiro.au)

Discussion Paper | Discussion Paper | Discussion Paper | Discussion Paper |

Impact of ocean acidification on our future climate

R. J. Matear and
A. Lenton

Abstract

Ocean acidification (OA) is the consequence of rising atmospheric CO_2, and it is occurring in conjunction with global warming. Observational studies show that OA will impact ocean biogeochemical cycles. Here, we use a coupled carbon-climate Earth System Model under the RCP8.5 emission scenario to evaluate and quantify the first-order impacts of OA on marine biogeochemical cycles and the potential feedback on our future climate over this century. We find that OA impacts have only a small impact on the future atmospheric CO_2 (less than 45 ppm) and future global warming (less than a 0.25 K) by 2100. While the climate change feedbacks are small, OA impacts may significantly alter the distribution of biological production and remineralization, which would alter the dissolved oxygen distribution in the ocean interior. Our results demonstrate that the consequences of OA will not be through its impact on climate change, but on how it impacts the flow of energy in marine ecosystems, which may significantly impact their productivity, composition and diversity.

1 Introduction

The oceans have taken up approximately a third of the total fossil fuel CO_2 emitted to the atmosphere since the onset of industrialization (140 ± 25 PgC, Khatiwala et al., 2009). This uptake has slowed the rate of global warming, but has led to detectable changes in the ocean chemistry (e.g. Doney et al., 2009). As the CO_2 enters the ocean, primarily through sea-air fluxes, it reacts with the sea water reducing the carbonate ion concentration and pH, collectively known as ocean acidification (OA). This uptake of anthropogenic CO_2 has reduced the pH of the modern ocean surface waters by 0.1 units or 30 % since pre-industrial times (Caldeira, 2005). By the end of this century, under the higher emission scenarios, the projected pH change since pre-industrial times maybe greater than 100 % (Orr et al., 2005).

OA has the potential to affect the major biogeochemical (BGC) cycles in the ocean (Gehlen et al., 2011), with potentially significant consequences for our future climate (Matear et al., 2010). In assessing the potential OA impacts on BGC cycles and climate, it is important to recognise that ocean acidification impacts do not occur in isolation, but they are associated with global warming, which may modulate their impacts (e.g. Brewer and Peltzer, 2009). Therefore, to assess the future impacts of OA requires an Earth System Model (ESM) that considers the interactive effects of global warming and OA on BGC cycling (Tagliabue et al., 2011). The goal of this study is to use a coupled-carbon ESM to evaluate and quantify the first-order impacts and climate feedbacks of OA. To do this, we first review the potential for ocean acidification to alter the major BGC cycles. We then use our ESM to assess how these modulations of the BGC by OA alter the projected climate in the current century. From our simulations, we then discuss how the OA modulated BGC changes affect the ocean environment. Finally, we end with a discussion of OA impacts on BGC cycling and climate that required further investigation.

2   Potential impacts on BGC cycles

Ocean acidification has the potential to modify marine BGC cycles in a number of ways, which could alter the future climate. We define the term BGC climate feedback, to denote an oceanic BGC process that may either enhance (positive feedback) or reduce (negative feedback) global warming due to rising greenhouse gases. For this study, we primarily focus on marine BGC processes that are impacted by OA and global warming, which can alter ocean uptake of carbon.

To aid the discussion of the potential impacts of OA on BGC cycles, we separate the impacts into processes that: (1) alter biological production in the photic zone; (2) alter the remineralization of sinking particulate organic and inorganic carbon in the ocean interior. These processes are summarised in Table 1, with an indication of the sign the impact has on the ocean storage of carbon based on published studies.

2.1 Biological production

The rising CO_2 in the upper ocean has the potential to affect biological production in several ways:

1. Increase net primary productivity by making photosynthesis more efficient (Rost et al., 2008). Experimental studies have also shown an increase in Particulate Organic Carbon (POC) production in response to increased levels of CO_2 (e.g. Zondervan et al., 2002).

2. Alter the stoichiometric nutrient to carbon ratio of the exported particulate organic matter, which enables ocean biology to partially overcome nutrient control on carbon production and export. Mesocosm experiments with natural plankton communities have reported an increased C/N ratio of particulate organic matter under elevated CO_2 (Riebesell et al., 2007; Bellerby et al., 2008). In these experiments, the C/N ratio increased from 6.0 at 350 µatm to 8.0 at about 1050 µatm. An increase in the C/N ratio of the export POC would result in increased storage of carbon in the ocean (Oschlies et al., 2008).

3. Impact the ability of organisms to calcify (Fabry et al., 2008), and this is anticipated to reduce the production of calcium carbonate. Due to the nature of the carbonate chemistry, reduced calcium carbonate production allows the upper ocean to increase its carbon uptake (Raven, 2005; Heinze, 2004; Hutchins, 2011).

All 3 of these affects would increase the storage of carbon in the ocean and provide a negative feedback to climate change.

2.2 Remineralization of particulate material

Most of the exported POC is remineralized in the upper 1000 m, but $\approx 10\%$ escapes to the deep ocean, where it is remineralized or buried in sediments, and sequestered from the atmosphere on millennium timescales Trull et al. (2001). Analysis of Particulate

Title Page

Abstract | Introduction

Conclusions | References

Tables | Figures

|◄ | ►|

◄ | ►

Back | Close

Full Screen / Esc

Printer-friendly Version

Interactive Discussion

Inorganic Carbon (PIC) and POC fluxes at water depths greater than 1000 m suggests a close association between these fluxes (Armstrong et al., 2002). The ratio of PIC production to POC is called the rain ratio (e.g. Archer et al., 2000). OA has the potential to impact the remineralization of sinking particulate material in the following ways:

5   1. Dissolution of $CaCO_3$ is an abiotic process driven by thermodynamics, and the rate of dissolution is related to the saturation state of the ocean (Orr et al., 2005). Chemical dissolution can occur when the saturation state of $CaCO_3$ falls below 1 (or below the lysocline). As the lysocline moves toward the surface with ocean acidification, increased dissolution of $CaCO_3$ sediments and sinking particles will 10   increase the alkalinity in the ocean (Ridgwell et al., 2009). This potentially increases the supply of alkalinity to the upper ocean increasing CO_2 uptake, which acts as a negative climate feedback

   2. Armstrong et al. (2002) proposed that $CaCO_3$ acts as a carrier for transporting POC to the deep ocean by ballasting the POC thereby increasing its sinking 15   speed. It is also hypothesised that the association between $CaCO_3$ and POC might protect the latter from bacterial degradation (Armstrong et al., 2002). If deepwater POC fluxes are controlled by $CaCO_3$, then a decrease in the $CaCO_3$ production would result in a decreased POC transport to the deep ocean. Consequently, POC would remineralise at shallower depths and therefore the net ef-20   ficiency of the biological pump would decrease, resulting in a positive climate change feedback.

   3. The remineralisation length scale of POC is dependent on microbal activity. It has been hypothesised that ocean acidification may increase the rate of microbial activity (Weinbauer et al., 2011), leading to more rapid remineralization of sink-25   ing POC, which would result in less carbon sequestration, and a positive climate change feedback.

In summary, changing the strength of the biological pump can have a feedback on climate change.

Impact of ocean acidification on our future climate

R. J. Matear and
A. Lenton

Full Screen / Esc

Printer-friendly Version

Interactive Discussion

3 Earth system model and simulations

3.1 Earth system model

For the simulations presented here a coupled carbon-climate earth system model was used (Mk3L-COAL). Mk3L-COAL includes a climate model, Mk3L (Phipps et al., 2011), coupled to a biogeochemical model of carbon, nitrogen and phosphorus cycles on land (CASA-CNP) in the Australian community land surface model, CABLE (Wang et al., 2010; Mao et al., 2011), and an ocean biogeochemical cycle model (Matear and Hirst, 2003; Duteil et al., 2012). The details of the ocean biogeochemical model are summarised in Appendix A.

The atmosphere model has a horizontal resolution of 5.6° by 3.2°, and 18 vertical layers. The land carbon model has the same horizontal resolution as the atmosphere. The ocean model has a resolution of 2.8° by 1.6°, and 21 vertical levels. Mk3L simulates the historical climate well, as compared to the models used for earlier IPCC assessments (Phipps et al., 2011; Pitman et al., 2011). Furthermore, the simulated response of the land carbon cycle to increasing atmospheric CO_2 and warming are consistent with those from the Coupled Model Intercomparison Project Phase 5 (CMIP5) (Zhang et al., 2013). The ocean biogeochemical model was shown to realistically simulate the global ocean carbon cycle (Duteil et al., 2012). Previous studies with this ocean biogeochemical model have shown it to realistically simulate anthropogenic carbon and CFC uptake by the ocean (Matsumoto et al., 2004). We referred to the ocean BGC formulation used in these previous studies as our standard BGC formulation, which is then modified to incorporate OA impacts.

The land model (CABLE) with CASA-CNP simulates the temporal evolution of heat, water and momentum fluxes at the surface, as well as, the biogeochemical cycles of carbon, nitrogen and phosphorus in plants and soils. For this study, we used the spatially explicit estimates of nitrogen deposition for 1990 (Dentener, 2006). The simulated (Zhang et al., 2013) geographic variations of nutrient limitations, major biogeochemical

fluxes and pools on the land under the present climate conditions are consistent with published studies (Wang et al., 2010; Hedin, 2004).

3.2 Model simulations

The ESM was spun-up under preindustrial atmospheric CO_2 (1850: 284.7 ppm) until the simulated climate became stable. Stability was defined as the linear trend of global mean surface temperature over the last 400 yr of the spin-up being less than 0.015 K per century.

For the historical period (1850–2005), the ESM was run using the historical atmospheric CO_2 concentrations as prescribed by the CMIP5 simulation protocol. For the historical period two simulations were performed. One, a Control simulation (CTRL) where atmospheric CO_2 only affects the carbon cycle and not the radiative properties of the atmosphere (Table 2). In the CTRL simulation there is no climate change due to greenhouse gas warming. Two, a Reference simulation (REF) where atmospheric CO_2 affects both the radiative properties of the atmosphere and the carbon cycle.

For the future, we used the RCP8.5 emissions scenario as provided by the CMIP5 (http://cmip-pcmdi.llnl.gov/cmip5/), and let our ESM, which has the full carbon-climate interactions determine the future atmospheric CO_2 concentrations (Zhang et al., 2013). The RCP8.5 scenario is the high CO_2 emissions scenario used in the IPCC's Fifth Assessment Report, and in this scenario radiative forcing increases to 8.5 W m^{-2} by 2100. For comparison, we also did a standard CMIP5 simulation where RCP8.5 atmospheric CO_2 concentrations were used rather than letting our ESM determine the future CO_2 concentrations from the emission scenario (we called this simulation RCP8.5). As discussed by Zhang et al. (2013), using RCP8.5 emissions rather than concentrations resulted in a slightly warmer world (0.25 K) by 2100, because of reduced land carbon uptake due to nutrient limitation. In all our simulations the vegetation distribution used (Lawrence et al., 2013) remained (unchanged) over the simulation period following the CMIP5 experimental design. Note, the CO_2 emissions from land use change were not included in our simulation but were taken into account in the emission estimates used

Impact of ocean acidification on our future climate

R. J. Matear and
A. Lenton

in the RCP8.5 emissions scenario. We also neglected changes in anthropogenic N deposition over the simulation period, because of the large uncertainty in the future deposition rate and the small impact it has on net land carbon uptake (Zaehle et al., 2010).

3.3 Ocean acidification impacts on BGC

To assess the potential impacts of OA on BGC cycles, we modified the ocean BGC formulation in the future period (2006–2100). These idealised modifications to the marine BGC cycle are summarised in Table 2 and described in more detail below. The modifications are designed to provide a first-order assessment of the OA impacts discussed in the previous section on the future climate.

The reference simulation (REF), refers to the standard BGC formulation with no OA impacts. With this ocean BGC formulation, the ESM simulates years 1850 to 2100 using historical atmospheric CO_2 for 1850 to 2006 and then the RCP8.5 emissions until year 2100. All of the remaining experiments to be discussed were started from year 2006 and use the same RCP8.5 emissions as the REF simulation.

The first OA simulation (EP+) considers the impact of rising CO_2 on the C/P ratio of the exported POC. The C/P changes are based on Oschlies et al. (2008), while the PIC export remains unchanged. The modified POC export (Q_{POC}) is given by the following equations where CO2 is the atmospheric CO_2 concentration and $J(P)$ is the phosphate uptake in the photic zone and Δz is the depth of the photic zone.

$$Q_{POC} = 106 \, J(P)F_o \, \Delta z \qquad (1)$$
$$F_o = 1 + (CO2 - 380) \cdot 2.3/700/6.6, \quad \text{for CO2} > 380 \qquad (2)$$

At the start of the experiment (2006), the atmospheric CO_2 equals 380 ppm and the scaling factor (F_o) is equal to 1, which is the value used in the REF experiment.

In the second OA experiment (EP++), in addition to the EP+ modification, the export of POC is prescribed to increase as atmospheric CO_2 levels rise reflecting the

enhanced production due to enhanced photosynthesis with increased CO_2. In addition the PIC export (Q_{PIC}) is prescribed to decline as $CaCO_3$ decreases with rising CO_2 (Ridgwell et al., 2009). To achieve this we increase the scaling factor on POC export (S_{npp}) and reduce the rain ratio between PIC and POC export (r) with atmospheric CO_2 as follows.

$$S_{npp} = S_{npp}^o[4.5 \cdot (CO2/380) - 3.5] \tag{3}$$

$$Q_{PIC} = r\,106\,J(P)\,\Delta z \tag{4}$$

$$r = r^o \cdot 1/(9.5 \cdot CO2/380 - 8.5) \tag{5}$$

where S_{npp}^o and r^o are the scaling factor and rain ratio respectively, used in the REF experiment. At an atmospheric CO_2 level of 1140 ppm (the approximate value at 2100) the scaling factor on POC export is 10 times and the rain ratio is 1/20 of the REF experiment. Note, that while the scaling factor was increased by 10 times the actual increase in export of POC is still constrained by the availability of phosphate and light, which dramatically reduces the increase in POC export in this experiment.

In the third OA simulation (Remin+), the standard BGC formulation is used but both the remineralization of POC and the dissolution of PIC are enhanced. The increased POC remineralization reflects an increasing rate of microbal activity with OA. The increased PIC dissolution reflects the impact of OA on the chemical dissolution of PIC. In the previously discussed experiments, POC and PIC have a prescribed depth profiles (see A10 and A11), which are now modified by the atmospheric CO_2 as follows to give an upper bound estimate of the potential impact of increased POC remineralization and increased PIC dissolution on carbon storage in the ocean. The following equations give the factors used to modify the prescribed depth profiles for POC and PIC from the REF experiment, where $Remin_{POC}^o = -0.9$ and $Remin_{PIC}^o = 3500$ in the REF simulation (see Eqs. A10 and A11).

$$Remin_{POC} = Remin_{POC}^o[1 + (CO2 - 380)/500] \tag{6}$$

$$Remin_{PIC} = Remin_{PIC}^o\,1/[1 + (CO2 - 380)/500] \tag{7}$$

With an atmospheric CO_2 level of 1000 ppm, the depth of remineralization declines by 2.25 from the REF experiment. For POC, this means the POC sinking below 200 m declines from 54 % in REF simulation to 25 %. For PIC, the PIC sinking below 1000 m reduces from 75 % in REF simulation to 37 %.

5   These BGC changes are an idealised representation of the OA impact on the ocean BGC cycle. They were deliberately chosen to provide extreme perturbations to the BGC cycle and test the potential for these impacts to have a significant consequence on the future projected climate.

4   Results and discussion

10 We will first discuss the REF simulation by assessing its present-day ocean state and its projected response to the RCP8.5 emission scenario. Then, we will discuss how OA impacts the ocean BGC cycle, and how this in turn impacts the future atmospheric CO_2 concentration and climate.

4.1   Historical period

15 For the historical period, the simulated global surface warming generally agrees with the observed warming (Fig. 1). The observed global surface temperature increase between 1850–1899 and 2001–2005 is 0.76 ± 0.19 K (Trenberth et al., 2007) compared to the simulated increase of 0.57 ± 0.07 K (Zhang et al., 2013). The observed land surface temperature increase from 1850–1899 to 2001–2005 is 1.0 ± 0.25 K (Brohan et al., 20 2006) compared to a simulated increase of 0.75 ± 0.06 K (Zhang et al., 2013).

Zhang et al. (2013) assessed the simulated anthropogenic CO_2 uptake by the land and ocean, and they showed that over the historical period the model realistically reflected the observed estimates. From 1850 to 2005, the total carbon accumulated in the land biosphere is 85 PgC, which is within the land carbon uptake of 135 ± 85 PgC 25 (Zhang et al., 2013) calculated from the estimated rates of ocean carbon uptake and at-

mospheric growth. The simulated carbon accumulated in the ocean (118 Pg C), agrees with the estimated anthropogenic carbon storage in the ocean of 135 ± 25 Pg C (Khatiwala et al., 2009). The simulated land and ocean carbon uptake is also consistent with the latest synthesis for the period 1960 to 2005 (Canadell et al., 2007).

To assess the realism of the ocean carbon simulation we compare: (1) dissolved oxygen at 500 m; (2) surface aragonite saturation state; (3) aragonite lysocline depth; and (4) the surface phosphate with the observations using a Taylor diagram (Fig. 2).

For dissolved oxygen at 500 m, the REF simulation is highly correlated with the observations (Boyer et al., 2009) (Fig. 2 and Table 3) with the simulation slightly overestimating the average oxygen concentration at 500 m. In general, the simulated dissolved oxygen levels at mid-depths are over-estimated, but the simulated thickness of suboxic water (defined as oxygen concentrations less than $5 \, \mu mol \, L^{-1}$) was about double the observed value.

For surface aragonite saturation state, the REF simulation is highly correlated with the aragonite saturation state calculated from the observations (Key et al., 2004), with the simulation slightly under-estimating the average saturation state (Fig. 3 and Table 3). In the ocean interior, the REF simulation has a similar pattern for the depth of the aragonite lysocline to the observations. In general, the simulated lysocline depth is a little deeper than observed, except in the Western Pacific where the simulated values are several hundred meters too deep (Fig. 3 and Table 3).

For surface phosphate, the REF simulation is highly spatially correlated with the observations (Boyer et al., 2009), but with slightly greater spatial variability (Fig. 2 and Table 3). The simulated mean surface phosphate concentration is also slightly less than observed.

In summary, the REF simulation generally reflects the present-day ocean state (correlation coefficient with the observations greater than 0.8). However, the important discrepancies with the observations are that the suboxic water is too thick and the lysocline in the Western Pacific subtropical and equatorial water is too deep. These

model biases need to be considered when assessing the projected regional changes associated with OA.

4.2 Future OA impacts on ocean BGC

4.2.1 Carbon climate feedbacks

The addition of the OA impacts on the ocean BGC alters the atmospheric CO_2 by less than 45 ppm by 2100 (Fig. 4). Enhanced POC export increases ocean carbon uptake, and atmospheric CO_2 drops by atmost 43 ppm by 2100. While the enhanced remineralization of the PIC and POC reduces carbon uptake, and atmospheric CO_2 increases by about 18 ppm by 2100. The combination of enhanced POC export with the shoaling of POC remineralization and PIC dissolution reduces atmospheric CO_2 by 38 ppm. The atmospheric CO_2 change in the COMB experiment is greater than the difference between EP++ and Remin+ simulations because the combination of larger export with shallower recycling of POC is more efficient at storing carbon in the ocean than when the two changes are considered separately. For the global climate, the OA impacts of these small atmospheric CO_2 changes causes the global surface temperature to deviate by less than 0.25 K (Fig. 4).

4.2.2 Changes in BGC fields

While the OA impacts on the ocean carbon storage and climate by the end of this century are small, we now investigate whether the BGC fields in the ocean are significantly altered by OA. Key ocean BGC fields that have been shown to be impacted by global warming and OA are aragonite saturation state, lysocline depth, export production, dissolved oxygen and volume of suboxic water. We focus on how the OA impacts each of these fields relative to the REF simulation.

4.2.3 Aragonite saturation state

For the surface aragonite saturation state, there are only subtle differences among the simulations (Fig. 5). As expected, all simulations show a dramatic reduction in the surface aragonite saturation state by 2100, with the surface water poleward of approx-
imately 40° S and 40° N being under-saturated with respect to aragonite (Fig. 5). At low latitudes, by 2100 the maximum aragonite saturation state from all simulations is less than 2.75, a level of saturation state that historically corals are not found (Guinotte et al., 2003). In all simulations, the upwelling region of the Eastern Equatorial Pacific shows a minimum in the tropical aragonite saturation state.

For the depth of the aragonite lysocline, all simulations show a dramatic shoaling in the polar regions (Fig. 6). In all simulations, the eastern tropical and subtropical Pacific lysocline is less than 100 m deep. Similarly, all simulations show lysocline depths of less than 100 m in the Indian Ocean. It is only in the equatorial western Pacific that the lysocline depths remain greater than 1000 m by the 2100. Note, this is the region, where the REF simulation over-estimated the lysocline depth by several hundred meters and in the OA experiments this region retains its resilience to change. This probably reflects a bias in the model, and it is anticipated that the region would show much greater shoaling by the end of the century (Bopp et al., 2013).

Overall the OA impacts only make subtle changes to the overall dramatic reduction in surface aragonite saturation state and lysocline depth projected with the RCP8.5 emission scenario.

4.2.4 Export production

For export of POC from the upper ocean, in the REF simulation there is a small global reduction (Fig. 7), which is mostly confined to the Equatorial Pacific, Indian Ocean and North Atlantic Oceans (Fig. 8). The export of PIC from the upper are also shown in Fig. 7, with all experiments showing a decline global export in the future except for REMIN+. In the REMIN+ simulation, the increase in POC export is associated

Title Page

Abstract	Introduction
Conclusions	References
Tables	Figures

◄ | ►|
◄ | ►

Back | Close

Full Screen / Esc

Printer-friendly Version

Interactive Discussion

with an increase in PIC export. Interestingly, the different OA experiments show large regional differences in export production (Fig. 8), with EP++ and REMIN+ substantially increasing export production in the Southern Ocean. However, for the global integrated value, OA impacts all cause an increase in POC export production, with the greatest increase occurring in the COMB projection.

The large range in the export production response of the different OA experiments is consistent with previous studies (e.g. Tagliabue et al., 2011). The simulations reveal that OA impacts on export production are much greater than their impacts on climate change. Such behaviour demonstrates the consequence of OA will not be through its impact on climate change, but on how it impacts the flow of energy in marine ecosystems. These changes may have significant affects on marine ecosystems and their productivity, biodiversity, and our future ability to exploit them as a food resource.

4.2.5 Dissolved oxygen

While the OA impacts had a small effect on atmospheric CO_2 levels, the export production varied dramatically amongst the simulations (Fig. 8), which has the potential to alter dissolved oxygen levels in the ocean. With climate change, the REF simulation shows a decline in the mid-water dissolve oxygen levels in the North Pacific, Equatorial Pacific and Southern Oceans (Fig. 9). The oceanic oxygen levels are expected to decline under global warming (e.g. Matear et al., 2000; Bopp et al., 2002), because surface warming lowers the sea surface oxygen concentrations, enhances stratification, reduces ventilation of the thermocline, and reduces thermohaline circulation, which all tend to decrease the supply of oxygen to the ocean interior. The reduce oxygen supply to the ocean interior is also linked to increased residence time of water at depth, thereby enhancing biological oxygen consumption in the ocean interior.

The REF simulation projects a global decline in total dissolved oxygen inventory of 1.8 % between 2006 and 2100 (Fig. 10b) and 2.5 % between 1850 and 2100. The projected small decline is comparable to other ESMs projections, which show a small decrease of 2 % to 4 % by the end of 2100 with climate change (Cocco et al., 2013). The

decline in dissolved oxygen in the major ocean basins is also reflected in a change in the thickness of the suboxic water (defined as water with dissolved oxygen of less than $5\,\mu mol\,L^{-1}$) (Fig. 10a). In the REF simulation, there is a projected 5 % decline in suboxic water by 2100 (Fig. 10a). This is consistent with the multi-model analysis (Cocco et al., 2013), which showed the projected total volume of suboxic waters remain relatively unchanged (±5 %) by the end of 2100 with climate change. As discussed by Cocco et al. (2013), the projected oxygen changes in the upper 1000 m of the ocean displayed a complex regional pattern with both positive and negative trends reflecting the complex interactions between changes in circulation, biological production, biological remineralization, and temperature.

The inclusion of OA impacts that could either increase POC export from the upper ocean (Fig. 7) and/or reduced its depth of remineralization may substantially decrease oxygen levels in the ocean interior. For the total oxygen inventory in the ocean, the simulations reveal that increased POC export causes a decline in oxygen while the shoaling of POC remineralization has little impact (Fig. 10b).

The EP+ simulation showed an increase in the thickness in the suboxic water of 17 % by 2100 (Fig. 10). Similar simulations where the C/N ratio of exported POC matter is increased with OA have projected reduce dissolved oxygen levels in the ocean and comparable values for the increase in the volume of suboxic water to the EP+ projection (Oschlies et al., 2008; Tagliabue et al., 2011).

Oschlies et al. (2008) showed the volume of suboxic water is very sensitive to small changes in the remineralization of POC in the ocean interior. Our simulations confirm this result, but also show the volume of suboxic water is sensitive to where OA increases POC export. With the shoaling of POC remineralization (REMIN+) there is a reduction in the volume of suboxic water. By confining POC remineralization to the upper ocean, the equatorial Pacific has less suboxic water, because this water is now more influenced by air–sea gas exchange and there is a global decline in the volume of suboxic water (Fig. 10). Similarly, the EP++ simulation with increased export production shows the greatest decline in total oxygen inventory (Fig. 10b), but a decline

in the volume of suboxic water by 2100 (Fig. 10a). The COMB simulation, with its increased POC export and shoaling of the POC remineralization also projects a decline in the volume of suboxic water. However, COMB simulation projects the development of suboxic zone in the North Pacific and Southern Ocean where the combination of
5 increased export production, shoaling of depth of POC remineralization, and increased stratification with global warming allows the develop of suboxic water in these regions.

The large uncertainty in the potential changes in POC export and remineralisation with OA, at present make it difficult to project the potential consequences of OA on dissolved oxygen levels with confidence, and this makes it a critical issue for further
10 investigation.

5 Summary and perspectives

Ocean acidification is the inevitable consequence of rising atmospheric CO_2 and occurs in conjunction with global warming. Published studies have hypothesised the potential of OA to impact biogeochemical cycling in the ocean. However, to date no stud-
15 ies have combined these impacts to quantify the integrated impacts on ocean biogeochemistry and the feedbacks to the future climate. Here, we explore the integrated consequences of these OA induced changes using a coupled carbon-climate ESM and some first-order representations of the potential OA impacts on marine biogeochemical cycles. A key result of this study is that OA does not significantly alter the
20 total carbon stored in the ocean, with the potential changes in atmospheric CO_2 levels (45 ppm maximum) being small compared to the future concentration projected with the RCP8.5 emission scenario by the end of this century (more than 1000 ppm). The small impact on the future atmospheric CO_2 means the OA impacts will have only a minor feedback on projected global warming, and our simulations suggest that by 2100 the
25 global averaged surface temperature would be altered by less than 0.25 K. Therefore, while the simulations do project significant global warming (≈ 3 K by 2100), the inclusion of OA impacts on the marine BGC cycle did not significantly alter the projected

changes. Consistent with both the small impact on carbon storage in the ocean and on global warming, the inclusion of OA impacts did not significantly alter the projected trajectory of future ocean acidification (e.g. surface aragonite state and lysocline depth). While the differences that occur by including OA impacts on biogeochemistry are small,

5 we emphasize with the RCP8.5 scenario by 2100 there will be significant changes in ocean acidification, that will impact the marine ecosystem. All polar surface waters will be under-saturated with respect to aragonite, and the maximum surface aragonite saturation state in the tropics will be less than 2.75, a value below which coral reefs are not historically found.

10 Where OA has the potential to have a significant impact is on the POC and PIC export from the upper ocean. We emphasize the consequence of these changes on marine ecosystems is highly uncertain and needs further study. While deliberately conceived to be large, the changes in PIC and POC export did not significantly change the future depth of the lysocline, however, they did significantly change the regional export

15 production and the interior oxygen levels.

The inclusion of OA impacts that could either increase POC export from the upper ocean or reduced its depth of remineralization could substantially decrease oxygen levels in the ocean interior. However, the large variability in potential changes in POC export with OA, at present make it difficult to confidently assess the consequences

20 of OA on dissolved oxygen levels and therefore this is another important issue to addressed. The decline in oxygen with the rising CO_2 could also have consequences for marine organisms with high metabolic rates. Global warming, lower oxygen and higher CO_2 levels represent physiological stresses for marine aerobic organisms that may act synergistically with ocean acidification (Portner and Farrell, 2008). Understanding how

25 OA and global warming impacts marine organisms warrants further investigation.

While CO_2 is the most important greenhouse gas modulated by the ocean, other greenhouse gases may be altered by OA. The next two most important greenhouse gas produced in the ocean are methane (CH_4) and nitrous oxide (N_2O), and their production in the ocean is linked to the remineralization of organic matter in low oxygen water

(Matear et al., 2010; Gruber and Galloway, 2008). The decline in the interior oxygen levels should be associated with increased production of both these gases (Glessmer et al., 2009). However, it is expected the response of CH_4 and N_2O would be less than the CO_2 impact shown here. Consistent with this conclusion, Schmittner et al. (2008) used an ESM climate change projection run until year 4000 to show the expansion of suboxic water doubled N_2O production in the ocean. The net result was an increase in atmospheric concentrations by 60 ppb that caused a warming of about 0.25 K, a small change given the length of their simulation.

Enhanced dinitrogen (N_2) fixation by cyanobacteria occurs under elevated pCO_2 concentrations (Hutchins et al., 2009). This provides an increased source of reactive nitrogen (N) and has the potential to increase primary production in the oligotrophic tropical and subtropical areas. However, this response is limited, as the relieving of N limitation will ultimate lead to phosphate limitation, which will limit the potential carbon uptake. Ocean-only simulations where sufficient N was added to remove nitrate limitation gave a maximum reduction in atmospheric CO_2 of about 22 ppm by 2100 (Matear and Elliott, 2004). Again, it is a small effect when compared to the future atmospheric value projected with the RCP8.5 emissions scenario.

Iron is a biologically important element, and therefore any change in its bioavailability has the potential to change the growth rate of phytoplankton. At present there is little consensus on the sign of this change with OA. A slower Fe uptake by diatoms with OA is seen in experiments with Atlantic surface water (Shi et al., 2010), while an increase has been reported in coastal waters (Breitbarth et al., 2010). If we assume OA can increase the bioavailablity of iron sufficiently to remove iron limitation on phytoplankton growth, we can use previous ocean model simulations to quantify the maximum potential increase in carbon storage. Such studies showed that this process alone could increased carbon storage in the ocean and reduce atmospheric CO_2 by 33 to 80 ppm by 2100 (Aumont and Bopp, 2006; Matear and Wong, 1999). While it is a larger response than what we project with our OA experiments, this is an upper bound of the potential feedback and it does not mechanistically link OA to the bioavailability of iron. Even this

upper bound estimate is small in comparison to the atmospheric CO_2 projected with the RCP8.5 emissions scenario by 2100 (≈ 1000 ppm), hence it would only have a minor impact on the future climate. We emphasize that the OA impact on the bioavailability of iron is how it may impact biological production in the ocean. Further, iron is only one

5 of many biologically important trace metals, for which their bioavailablility will change in response to OA (Hoffmann et al., 2012) and potentially alter biological production. Therefore, more studies are required to understand how changes in the bioavailability of trace metals in response to OA may impact future biological production.

The ocean is also a source of climatically active trace gases to the atmosphere like

10 dimethyl sulphide (DMS), which can alter cloud properties. DMS is a gaseous sulphur compound produced by marine biota in surface seawater (Gabric et al., 1993). The marine production of DMS provides 90 % of the biogenic sulfur in the marine atmosphere, and in the atmosphere it is rapidly oxidised to produce particles that can affect cloud formation and climate (Arnold et al., 2013). The effects of increasing anthropogenic

15 CO_2 and the resulting warming and ocean acidification on trace gas production in the oceans are poorly understood.

Modelling studies vary substantially in their predictions of the change in DMS emissions with climate change. Elevating CO_2 in isolation of other environmental change suggested a significant decrease in the future concentration of DMS (Hopkins et al.,

20 2011). However, studies in polar waters suggested increases in DMS emission ranging from 30 % to more than 150 % (Cameron-Smith et al., 2011; Kloster et al., 2007; Gabric et al., 2011) by 2100 with only climate change. While a recent ESM study by Six et al. (2013) projected by 2100 a global decrease in DMS production of 18 ± 3 %, with 83 % of this change attributed to OA, leading to only a modest warming of 0.23 to 0.48 K. Six

25 et al. (2013) simulated strong regional responses of increasing (polar regions) and decreasing DMS emissions, which reflected the combined affect of increased net primary production and regional shifts in community composition. Therefore, more studies combining the impacts of global warming and OA on marine DMS production are warranted

to better determine its regional response and sign, particularly at the marine species and ecosystem levels.

Potential climate-carbon feedbacks of OA and global warming appear small relative to the huge input of carbon into the atmosphere by human activity. However, understanding and projecting the combined OA and global warming impact on marine ecosystems remains the outstanding issue to tackle. In particular, biological production may change with the projected OA, and the potential consequences for marine organisms and ecosystems are poorly known.

Appendix A

Ocean biogeochemical model equations

The ocean BGC module is based on Matear and Hirst (2003), and simulates the evolution of phosphate (P), oxygen (O), carbon (C) and alkalinity (A) in the ocean. The following briefly summarises the how the BGC processes in the ocean interior are parameterised and how they affect the 4 BGC tracers.

In the photic zone, which is set to be the surface layer of the model (upper 50 m), the biological production of particulate organic and inorganic matter occurs. For particulate organic matter, the production of particulate organic phosphorus (POP) was defined by the following equations:

Impact of ocean acidification on our future climate

R. J. Matear and A. Lenton

$$V_{max} = 0.6(1.066)^T \tag{A1}$$

$$F(I) = [1 - e^{R(I)}] \tag{A2}$$

$$R(I) = \frac{I(x,t)\alpha PAR}{V_{max}} \tag{A3}$$

$$J(P) = S_{npp} V_{max} \text{Min}\left[\frac{P}{P + P_k}, F(I)\right]\Delta z \tag{A4}$$

V_{max} is the maximum growth rate in day^{-1}, which is a function of the surface layer temperature (T, °C). $F(I)$ is the productivity vs. irradiance equation used to describe phytoplankton growth, which is given as a unitless value and provides a measure of light limited growth. $R(I)$ a units less function of the light availability for growth, which is calculated from the incident short wave radiation (I) in W m^{-2}), the fraction of short wave radiation that is photosynthetically active PAR (unitless factor), and the initial slope (α) of the productivity vs. radiance curve for phytoplankton growth (day^{-1} (W m^{-2})$^{-1}$). $J(P)$ gives the uptake of phosphate by POP production in mmol P m^{-2} day^{-1} in the photic zone. $J(P)$ is a function of the scaling parameter (S_{npp}) in mmol P m^{-3}, the thickness of the surface layer (Δz) in metres and the growth limitation function. The value S_{npp} was set to 0.005 where it satisfactorily reproduced the observed phosphate and oxygen concentrations. The growth limitation function uses the minimum value of light and phosphate limited growth. The phosphate limited growth term is based on the phosphate concentration of the surface layer P and the half saturation uptake (P_k) value for phosphate utilisation, which was set to 0.1 mmol P m^{-3}.

The POP production in the photic zone was linked to inorganic carbon, oxygen and alkalinity uptake in the photic zone by the following equations:

$$J(C) = 106 \, J(P) \tag{A5}$$

$$J(O) = -136 \, J(P) \tag{A6}$$

$$J(A) = -16 \, J(P) \tag{A7}$$

PIC production in the model was linked to POC production by using a fixed rain ratio (r) of 9 % (Yamanaka and Tajika, 1996) to give the following uptake of inorganic carbon and alkalinity in the photic zone:

$$K(C) = r \times 106 \, J(P) \tag{A8}$$

$$K(A) = r \times 2 \times 106 \, J(P), \quad r = 0.09 \tag{A9}$$

The POC and PIC produced in the photic zone was instantaneously remineralised in the ocean interior above where it was produced. The POC ($J(C) \times \Delta z$) and PIC ($K(C) \times \Delta z$) production in the photic zone was remineralised in the ocean interior using the following depth profiles of POC and PIC:

$$POC(z) = \frac{z}{100\,\text{m}}^{\text{Remin}_{POC}} \tag{A10}$$

$$PIC(z) = \exp(z/\text{Remin}_{PIC}) \tag{A11}$$

where z is depth in meters, $\text{Remin}_{POC} = -0.9$ sets the reminalisation length scale of POC and $\text{Remin}_{PIC} = 3500\,\text{m}$ sets the depth scale for PIC dissolution (Yamanaka and Tajika, 1996). From the POC and PIC depth profiles, the production of inorganic carbon from the remineralisation of POC (C_o) and the dissolution of PIC (C_i) is given by:

$$C_o(z) = -J(C) \times \Delta z \times \frac{d}{dz} POC(z) \tag{A12}$$

$$C_i(z) = -K(C) \times \Delta z \times \frac{d}{dz} PIC(z) \tag{A13}$$

with no remineralisation above 100 m and all the POC and PIC reaching the ocean bottom remineralised in the bottom layer of the model.

Impact of ocean acidification on our future climate

R. J. Matear and A. Lenton

Title Page

Abstract | Introduction

Conclusions | References

Tables | Figures

◀ | ▶

◀ | ▶

Back | Close

Full Screen / Esc

Printer-friendly Version

Interactive Discussion

References

Archer, D. E., Eshel, G., Winguth, A., Broecker, W., Pierrehumbert, R., Tobis, M., and Jacob, R.: Atmospheric pCO$_2$ sensitivity to the biological pump in the ocean, Global Biogeochem. Cy., 14, 1219–1230, 2000. 17687

Armstrong, R. A., Lee, C., Hedges, J. I., Honjo, S., and Wakeham, S. G.: A new, mechanistic model for organic carbon fluxes in the ocean based on the quantitative association of POC with ballast minerals, Deep-Sea Res. Pt. II, 49, 219–236, 2002. 17687

Arnold, H. E., Kerrison, P., and Steinke, M.: Interacting effects of ocean acidification and warming on growth and DMS-production in the haptophyte coccolithophore Emiliania huxleyi, Glob. Change Biol., 19, 1007–1016, doi:10.1111/gcb.12105, 2013. 17701

Aumont, O. and Bopp, L.: Globalizing results from ocean in situ iron fertilization studies, Global Biogeochem. Cy., 20, GB2017, doi:10.1029/2005GB002591, 2006. 17700

Bellerby, R. G. J., Schulz, K. G., Riebesell, U., Neill, C., Nondal, G., Heegaard, E., Johannessen, T., and Brown, K. R.: Marine ecosystem community carbon and nutrient uptake stoichiometry under varying ocean acidification during the PeECE III experiment, Biogeosciences, 5, 1517–1527, doi:10.5194/bg-5-1517-2008, 2008. 17686

Bopp, L., Quere, C. L., Heimann, M., Manning, A. C., and Monfray, P.: Climate-induced oceanic oxygen fluxes: implications for the contemporary carbon budget, Global Biogeochem. Cy., 16, 1022, doi:10.1029/2001GB001445, 2002. 17696

Bopp, L., Resplandy, L., Orr, J. C., Doney, S. C., Dunne, J. P., Gehlen, M., Halloran, P., Heinze, C., Ilyina, T., Séférian, R., Tjiputra, J., and Vichi, M.: Multiple stressors of ocean ecosystems in the 21st century: projections with CMIP5 models, Biogeosciences, 10, 6225–6245, doi:10.5194/bg-10-6225-2013, 2013. 17695

Boyer, T. P., Antonov, J. I., Baranova, O. K., Garcia, H. E., Johnson, D. R., Locarnini, R. A., Mishonov, A. V., O'Brien, T., Seidov, D., and Smolyar, I. V.: World Ocean Database 2009, edited by: Levitus, S., NOAA Atlas NESDIS 66, US Gov. Printing Office, Wash, DC, 216 pp., 2009. 17693, 17715

Breitbarth, E., Bellerby, R. J., Neill, C. C., Ardelan, M. V., Meyerhöfer, M., Zöllner, E., Croot, P. L., and Riebesell, U.: Ocean acidification affects iron speciation during a coastal seawater mesocosm experiment, Biogeosciences, 7, 1065–1073, doi:10.5194/bg-7-1065-2010, 2010. 17700

Impact of ocean acidification on our future climate

R. J. Matear and A. Lenton

Title Page

Abstract	Introduction
Conclusions	References
Tables	Figures

Back | Close

Full Screen / Esc

Printer-friendly Version

Interactive Discussion

Brewer, P. G. and Peltzer, E. T.: Oceans: limits to marine life, Science, 324, 347–348, 2009. 17685

Brohan, P., Kennedy, J. J., Harris, I., Tett, S. F. B., and Jones, P. D.: Uncertainty estimates in regional and global observed temperature changes: a new data set from 1850, J. Geophys. Res.-Atmos., 111, D12106, doi:10.1029/2005JD006548, 2006. 17692

Caldeira, K.: Ocean model predictions of chemistry changes from carbon dioxide emissions to the atmosphere and ocean, J. Geophys. Res., 110, C09S04, doi:10.1029/2004JC002671, 2005. 17684

Cameron-Smith, P., Elliott, S., Maltrud, M., Erickson, D., and Wingenter, O.: Changes in dimethyl sulfide oceanic distribution due to climate change, Geophys. Res. Lett., 38, L07704, doi:10.1029/2011GL047069, 2011. 17701

Canadell, J. G., Le Quere, C., Raupach, M. R., Field, C. B., Buitenhuis, E. T., Ciais, P., Conway, T. J., Gillett, N. P., Houghton, R. A., and Marland, G.: Contributions to accelerating atmospheric CO_2 growth from economic activity, carbon intensity, and efficiency of natural sinks, Proc. Natl. Acad. Sci. USA, 104, 18866–18870, 2007. 17693

Cocco, V., Joos, F., Steinacher, M., Frölicher, T. L., Bopp, L., Dunne, J., Gehlen, M., Heinze, C., Orr, J., Oschlies, A., Schneider, B., Segschneider, J., and Tjiputra, J.: Oxygen and indicators of stress for marine life in multi-model global warming projections, Biogeosciences, 10, 1849–1868, doi:10.5194/bg-10-1849-2013, 2013. 17696, 17697

Dentener, F.: Global maps of atmospheric nitrogen deposition, 1860, 1993, and 2050, Data set, available at: http://daac.ornl.gov/ from Oak Ridge National Laboratory Distributed Active Archive Center, Oak Ridge, Tennessee, USA, 2006. 17688

Doney, S. C., Fabry, V. J., Feely, R. A., and Kleypas, J. A.: Ocean acidification: the other CO_2 problem, Annu. Rev. Mar. Sci., 1, 169–192, 2009. 17684

Duteil, O., Koeve, W., Oschlies, A., Aumont, O., Bianchi, D., Bopp, L., Galbraith, E., Matear, R., Moore, J. K., Sarmiento, J. L., and Segschneider, J.: Preformed and regenerated phosphate in ocean general circulation models: can right total concentrations be wrong?, Biogeosciences, 9, 1797–1807, doi:10.5194/bg-9-1797-2012, 2012. 17688

Fabry, V., Seibel, B., Feely, R., and Orr, J.: Impacts of ocean acidification on marine fauna and ecosystem processes, ICES J. Mar. Sci. 65, 414–432, 2008. 17686

Gabric, A., Murray, N., Stone, L., and Kohl, M.: Modelling the proeduction of dimethylsulfide during a phytoplankton bloom, J. Geophys. Res., 98, 22805–22816, 1993. 17701

Gabric, A., Qu, B., Matrai, P., and Hirst, A.: The simulated response of dimethylsulfide production in the Arctic Ocean to global warming, Tellus B, 57, 391–403, 2011. 17701

Gehlen, M., Gruber, N., Gangstø, R., Bopp, L., and Oschlies, A.: Biogeochemical consequences of ocean acidification and feedbacks to the earth system, in: Ocean Acidification, vol. 1, edited by: Gattuso, J.-P. and Hansson, L., 230–248, Oxford University Press, 2011. 17685

Glessmer, M. S., Eden, C., and Oschlies, A.: Contribution of oxygen minimum zone waters to the coastal upwelling off Mauritania, Prog. Oceanogr., 83, 143–150, 2009. 17700

Gruber, N. and Galloway, J.: An earth-system perspective of the global nitrogen cycle, Nature, 451, 293–296, 2008. 17700

Guinotte, J. M., Buddemeier, R. W., and Kleypas, J. A.: Future coral reef habitat marginality: temporal and spatial effects of climate change in the Pacific basin, Coral Reefs, 22, 551–558, doi:10.1007/s00338-003-0331-4, 2003. 17695

Hedin, L. O.: Global organization of terrestrial plant–nutrient interactions, Proc. Natl. Acad. Sci. USA, 101, 10849–10850, 2004. 17689

Heinze, C.: Simulating oceanic $CaCO_3$ export production in the greenhouse, Geophys. Res. Lett., 31, L16308, doi:10.1029/2004GL020613, 2004. 17686

Hoffmann, L. J., Breitbarth, E., Boyd, P. W., and Hunter, K. A.: Influence of ocean warming and acidification on trace metal biogeochemistry, Mar. Ecol.-Prog. Ser., 470, 191–205, doi:10.3354/meps10082, 2012. 17701

Hopkins, F., Nightingale, P., and Liss, P.: Effects of ocean acidification on the marine source of atmospherically active trace gases, in: Ocean Acidification, edited by: Gattuso, J.-P. and Hansson, L., p. 210, Oxford University Press, 2011. 17701

Hutchins, D. A.: Oceanography: forecasting the rain ratio, Nature, 476, 41–42, 2011. 17686

Hutchins, D. A., Mulholland, M. R., and Fu, F.: Nutrient cycles and marine microbes in a CO_2-enriched ocean, Oceanography, 22, 128–145, 2009. 17700

Key, R. M., Kozyr, A., Sabine, C. L., Lee, K., Wanninkhof, R., Bullister, J. L., Feely, R. A., Millero, F. J., Mordy, C., and Peng, T. H.: A global ocean carbon climatology: Results from Global Data Analysis Project (GLODAP), Global Biogeochem. Cy., 18, GB4031, doi:10.1029/2004GB002247, 2004. 17693, 17716

Khatiwala, S., Primeau, F., and Hall, T.: Reconstruction of the history of anthropogenic CO_2 concentrations in the ocean, Nature, 462, 346–349, 2009. 17684, 17693

Title Page

Abstract | Introduction

Conclusions | References

Tables | Figures

◄ | ►

◄ | ►

Back | Close

Full Screen / Esc

Printer-friendly Version

Interactive Discussion

Kloster, S., Six, K. D., Feichter, J., Maier-Reimer, E., Roeckner, E., Wetzel, P., Stier, P., and Esch, M.: Response of dimethylsulfide (DMS) in the ocean and atmosphere to global warming, J. Geophys. Res., 112, G03005, doi:10.1029/2006JG000224, 2007. 17701

Lawrence, P. J., Feddema, J. J., Bonan, G. B., Meehl, G. A., O'Neill, B. C., Oleson, K. W., Levis, S., Lawrence, D. M., Kluzek, E., Lindsay, K., and Thornton, P. E.: Simulating the biogeochemical and biogeophysical impacts of transient land cover change and wood harvest in the Community Climate System Model (CCSM4) from 1850 to 2100, J. Climate, 25, 3071–3095, 2013. 17689

Mao, J., Phipps, S. J., Pitman, A. J., Wang, Y. P., Abramowitz, G., and Pak, B.: The CSIRO Mk3L climate system model v1.0 coupled to the CABLE land surface scheme v1.4b: evaluation of the control climatology, Geosci. Model Dev., 4, 1115–1131, doi:10.5194/gmd-4-1115-2011, 2011. 17688

Matear, R. J. and Elliott, B.: Enhancement of oceanic uptake of anthropogenic CO_2 by macronutrient fertilization, J. Geophys. Res., 109, C4001, doi:10.1029/2000JC000321, 2004. 17700

Matear, R. J. and Hirst, A. C.: Long term changes in dissolved oxygen concentrations in the ocean caused by protracted global warming, Global Biogeochem. Cy., 17, 1125, doi:10.1029/2002GB001997, 2003. 17688, 17702

Matear, R. J. and Wong, C. S.: Potential to increase the oceanic CO_2 uptake by enhancing marine productivity in high nutrient low chlorophyll regions, 249–253, 1999. 17700

Matear, R. J., Hirst, A. C., and McNeil, B. I.: Changes in dissolved oxygen in the Southern Ocean with climate change, Geochem. Geophys. Geosys., 1, 1050, doi:10.1029/2000GC000086, 2000. 17696

Matear, R. J., Wang, Y.-P., and Lenton, A.: Land and ocean nutrient and carbon cycle interactions, Curr. Op. Environ. Sustain., 2, 258–263, 2010. 17685, 17700

Matsumoto, K., Sarmiento, J. L., Key, R. M., Aumont, O., Bullister, J. L., Caldeira, K., Campin, J. M., Doney, S. C., Drange, H., Dutay, J. C., Follows, M. J., Gao, Y., Gnanadesikan, A., Gruber, N., Ishida, A., Joos, F., Lindsay, K., Maier-Reimer, E., Marshall, J. C., Matear, R. J., Monfray, P., Mouchet, A., Najjar, R., Plattner, G. K., Schlitzer, R., Slater, R., Swathi, P. S., Totterdell, I. J., Weirig, M. F., Yamanaka, Y., Yool, A., and Orr, J. C.: Evaluation of ocean carbon cycle models with data-based metrics, Geophys. Res. Lett., 31, L07303, doi:10.1029/2003GL018970, 2004. 17688

Orr, J. C., Fabry, V. J., Aumont, O., Bopp, L., Doney, S. C., Feely, R. A., Gnanadesikan, A., Gruber, N., Ishida, A., Joos, F., Key, R. M., Lindsay, K., Maier-Reimer, E., Matear, R. J., Monfray, P., Mouchet, A., Najjar, R. G., Plattner, G. K., Rodgers, K. B., Sabine, C. L., Sarmiento, J. L., Schlitzer, R., Slater, R. D., Totterdell, I. J., Weirig, M. F., Yamanaka, Y., and Yool, A.: Anthropogenic ocean acidification over the twenty-first century and its impact on calcifying organisms, Nature, 437, 681–686, 2005. 17684, 17687

Oschlies, A., Schulz, K. G., Riebesell, U., and Schmittner, A.: Simulated 21st century's increase in oceanic suboxia by CO_2-enhanced biotic carbon export, Global Biogeochem. Cy., 22, GB4008, doi:10.1029/2007GB003147, 2008. 17686, 17690, 17697

Phipps, S. J., Rotstayn, L. D., Gordon, H. B., Roberts, J. L., Hirst, A. C., and Budd, W. F.: The CSIRO Mk3L climate system model version 1.0 – Part 1: Description and evaluation, Geosci. Model Dev., 4, 483–509, doi:10.5194/gmd-4-483-2011, 2011. 17688

Pitman, A. J., Avila, F. B., Abramowitz, G., Wang, Y. P., Phipps, S. J., and de Noblet-Ducoudré, N.: Importance of background climate in determining impact of land-cover change on regional climate, Nat. Clim. Change, 1, 472–475, 2011. 17688

Portner, H. O. and Farrell, A. P.: ECOLOGY: physiology and climate change, Science, 322, 690–692, doi:10.1126/science.1163156, 2008. 17699

Raven, J. A.: Ocean Acidification Due to Increasing Atmospheric Carbon Dioxide, R Society (Great Britain), 60 pp., 2005. 17686

Ridgwell, A., Schmidt, D. N., Turley, C., Brownlee, C., Maldonado, M. T., Tortell, P., and Young, J. R.: From laboratory manipulations to Earth system models: scaling calcification impacts of ocean acidification, Biogeosciences, 6, 2611–2623, doi:10.5194/bg-6-2611-2009, 2009. 17687, 17691

Riebesell, U., Schulz, K. G., Bellerby, R. G. J., Botros, M., Fritsche, P., Meyerhofer, M., Neill, C., Nondal, G., Oschlies, A., Wohlers, J., and Zollner, E.: Enhanced biological carbon consumption in a high CO_2 ocean, Nature, 450, 545–549, 2007. 17686

Rost, B., Zondervan, I., and Wolf-Gladrow, D.: Sensitivity of phytoplankton to future changes in ocean carbonate chemistry: current knowledge, contradictions and research directions, Mar. Ecol.-Prog. Ser., 373237., 227, 227–237, 2008. 17686

Schmittner, A., Oschlies, A., Matthews, H. D., and Galbraith, E. D.: Future changes in climate, ocean circulation, ecosystems, and biogeochemical cycling simulated for a business-as-usual CO_2 emission scenario until year 4000 AD, Global Biogeochem. Cy., 22, GB1013, doi:10.1029/2007GB002953, 2008. 17700

Impact of ocean acidification on our future climate

R. J. Matear and A. Lenton

Shi, D., Xu, Y., Hopkinson, B., and Morel, F.: Effect of ocean acidification on iron availability to marine phytoplankton, Science, 327, 676, doi:10.1126/science.1183517,, 2010. 17700

Six, K. D., Kloster, S., Ilyina, T., Archer, S. D., Zhang, K., and Maier-Reimer, E.: Global warming amplified by reduced sulphur fluxes as a result of ocean acidification, Nat. Clim. Change, 3, 1–4, 2013. 17701

Tagliabue, A., Bopp, L., and Gehlen, M.: The response of marine carbon and nutrient cycles to ocean acidification: large uncertainties related to phytoplankton physiological assumptions, Global Biogeochem. Cy., 25, GB3017, doi:10.1029/2010GB003929, 2011. 17685, 17696, 17697

Trenberth, K. E., Jones, P. D., Ambenje, P., Bojariu, R., Easterling, D., Tank, A. K., Parker, D., Rahimzadeh, F., Renwick, J. A., Rusticucci, M., Soden, B., and Zhai, P.: Observations: Surface and Atmospheric Climate Change, 2007. 17692

Trull, T. W., Bray, S. G., Manganini, S. J., Honjo, S., and Francois, R.: Moored sediment trap measurements of carbon export in the Subantarctic and Polar Frontal Zones of the Southern Ocean, south of Australia, J. Geophys. Res.-Atmos., 106, 31489–31509, 2001. 17686

Wang, Y. P., Law, R. M., and Pak, B.: A global model of carbon, nitrogen and phosphorus cycles for the terrestrial biosphere, Biogeosciences, 7, 2261–2282, doi:10.5194/bg-7-2261-2010, 2010. 17688, 17689

Weinbauer, M. G., Mari, X., and Gattuso, J.-P.: Effects of ocean acidification on the diversity and activity of heterotrophic marine microorganisms, 2011. 17687

Yamanaka, Y. and Tajika, E.: The role of the vertical fluxes of particulate organic matter and calcite in the oceanic carbon cycle: studies using a ocean biogeochemical general circulation model, Global Biogeochem. Cy., 10, 361–382, 1996. 17704

Zaehle, S., Friedlingstein, P., and Friend, A. D.: Terrestrial nitrogen feedbacks may accelerate future climate change, Geophys. Res. Lett., 37, L01401, doi:10.1029/2009GL041345, 2010. 17690

Zhang, Q. N., Wang, Y.-P., Matear, R. J., Pitman, A. J., and Dai, Y. J.: Nitrogen and phosphorous limitations significantly reduce future allowable CO_2 emissions, P. Natl. Acad. Sci. USA, in review, 2013. 17688, 17689, 17692, 17714

Zondervan, I., Rost, B., and Riebesell, U.: Effect of CO_2 concentration on the PIC/POC ratio in the coccolithophore Emiliania huxleyi grown under light-limiting conditions and different daylengths, J. Exp. Mar. Biol. Ecol., 272, 55–70, 2002. 17686

Impact of ocean acidification on our future climate

R. J. Matear and
A. Lenton

Title Page

Abstract | Introduction

Conclusions | References

Tables | Figures

◄ | ►

Back | Close

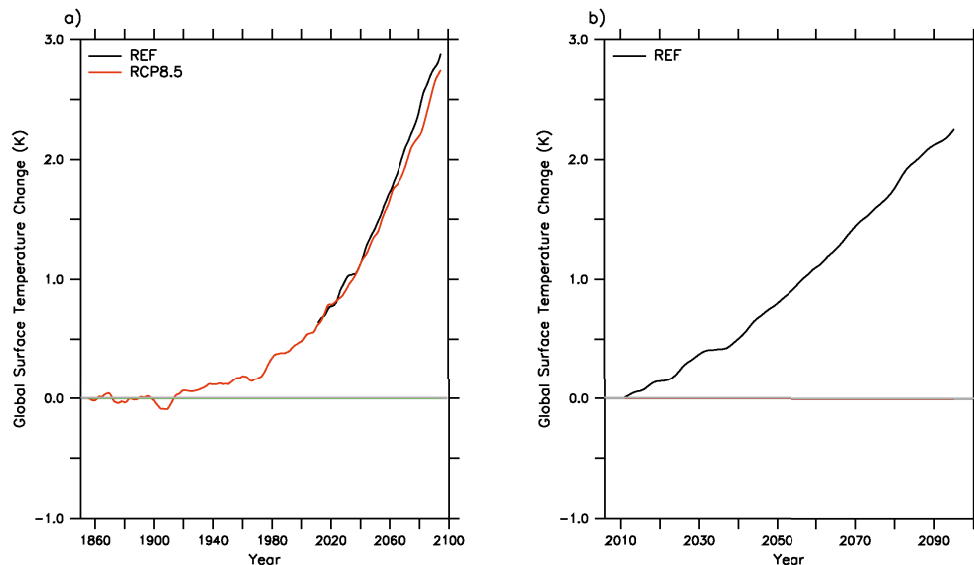Full Screen / Esc

Printer-friendly Version

Interactive Discussion

Table 1. Potential Ocean Acidification impacts on BGC cycles. The sign column denotes the impact on future climate with a positive value reflecting greater climate change (positive feedback).

Biological Production Process	Impact on climate change
Increased net primary productivity	–
Increased export of organic matter	–
Increased C/N ratio of organic matter	–
Reduced Calcification	–
Remineralization of Sinking Organic Matter Process	Impact on climate change
Increasing microbial POC remineralization	+
Reduced Ballasting with Calcium Carbonate	+

Table 2. Summary of the ocean BGC experiments presented in this study. In the CRTL simulation, only the land and ocean carbon components of the ESM see the rising atmosphere CO_2, while the radiation properties of the atmosphere stay fixed at the pre-industrial atmospheric CO_2 level of 284.7 ppm. In the remaining simulations, both the climate and the carbon components experience the impact of rising atmospheric CO_2. The RCP8.5 simulation uses the prescribed atmospheric CO_2 as provided by the CMIP5 for this scenario. The REF simulation starts in 1850 using historical atmospheric CO_2 and switches to the RCP8.5 future emissions scenario at the start of 2006. The 4 other simulations (EP+, EP++, REMIN+ and COMB) start from the REF simulation at the end of 2005 and go until 2100 using the RCP8.5 future emissions. Please refer to the text for a description of how BGC cycle is modified in the EP+, EP++, REMIN+ and COMB simulations.

Name	Description	Duration
CTRL	Standard BGC with historical and RCP8.5 atmospheric CO_2 but with no climate change	1850–2100
RCP8.5	Standard BGC with historical atmospheric CO_2 and RCP8.5 future atmosphere CO_2	1850–2100
REF	Standard BGC with historical atmospheric CO_2 and RCP8.5 future emissions	1850–2100
EP+	Increased C/P ratio of POC export and reduced PIC as CO_2 increased	2006–2100
EP++	EP+ and increased POC export as CO_2 increased	2006–2100
REMIN+	Increased rate of POC and PIC remineralization as CO_2 increased	2006–2100
COMB	Combined affect of EP++ and REMIN+	2006–2100

Table 3. Summary statistics of the comparison of the REF 1995 simulated fields with the observations shown in Fig. 2.

Field	Observed Average	Simulated Average	Observed σ	Observations vs. REF simulation in 1995					Correlation Coefficent
				Normalized					
				Mean Error	RMS'	RMS	σ		
Phosphate at 0 m (μmol L^{-1})	0.51	0.44	0.49	−0.13	0.58	0.60	1.25		0.89
Oxygen at 500 m (μmol L^{-1})	147.6	190.1	75.8	0.56	0.57	0.80	1.06		0.85
Aragonite Saturation State at 0 m	3.01	2.75	0.84	−0.31	0.36	0.47	1.09		0.95
Lysocline Depth (m)	1051.4	1414.5	717.6	0.51	0.61	0.79	1.02		0.81

Fig. 1. (a) Simulated change in global surface temperature using the historical and RCP8.5 atmospheric CO_2 concentration (Zhang et al., 2013), and using the RCP8.5 emission scenario (REF). In the REF simulation, the future emissions are prescribed (based on the RCP8.5 scenario) and our ESM determines the future atmospheric CO_2 concentration. While the RCP8.5 simulation uses the atmospheric CO_2 concentrations generated by Integrated Assessment Model to provide a standardised future atmospheric CO_2 concentrations for CMIP5. **(b)** Simulated global surface temperature change for the future period from the REF simulation.
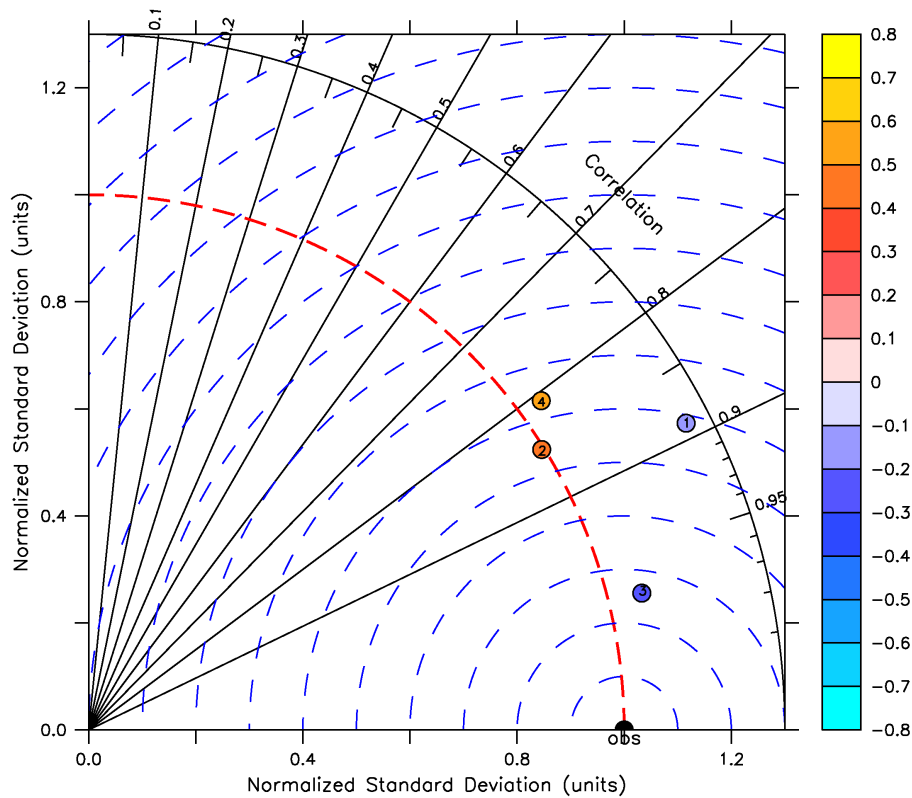
Fig. 2. Taylor diagram of the comparison of the simulated fields with the observations for surface phosphate (1), dissolved oxygen at 500 m (2) (Boyer et al., 2009), surface aragonite saturation state (3) and lysocline depth (4). The colour bar gives the bias in the simulated fields normalised by the standard deviation in the observed field.
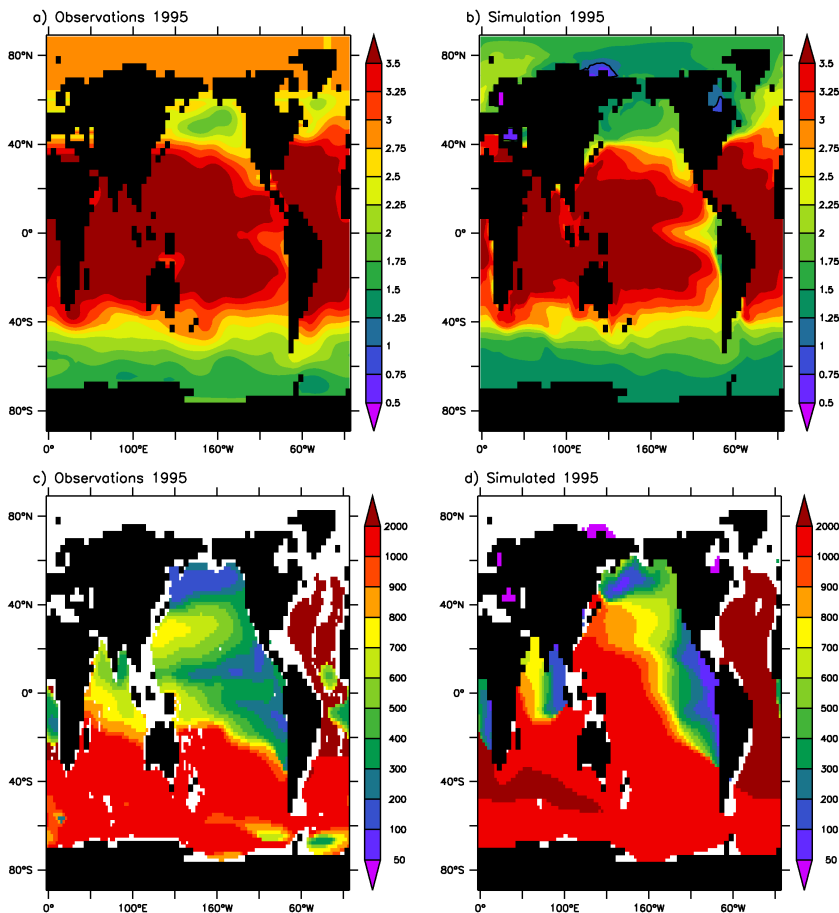
Fig. 3. Annual mean comparison of the observed and simulated fields for **(a–b)** surface arago-
nite saturation state **(c–d)** aragonite lysocline depth (m) The observations for aragonite satura-
tion come from Key et al. (2004).
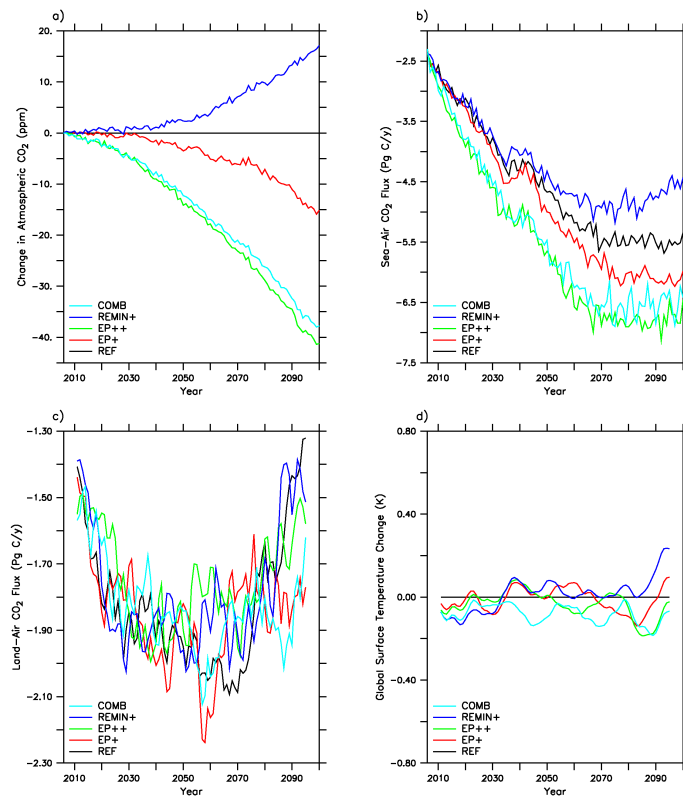
Fig. 4. (a) Change in atmospheric CO_2 (ppm) for the future period relative to the REF simulation for the various OA experiments (see Table 2 for a description of the experiments). **(b)** Simulated global ocean carbon uptake for the different OA experiments. **(c)** Simulated 10 yr running mean of the land carbon uptake by the different OA experiments. **(d)** Simulated 10 yr running mean of the change in global surface temperature relative to the REF simulation for the various OA experiments.

Title Page

Abstract | Introduction

Conclusions | References

Tables | Figures

|◄ | ►|

◄ | ►

Back | Close

Full Screen / Esc

Printer-friendly Version

Interactive Discussion
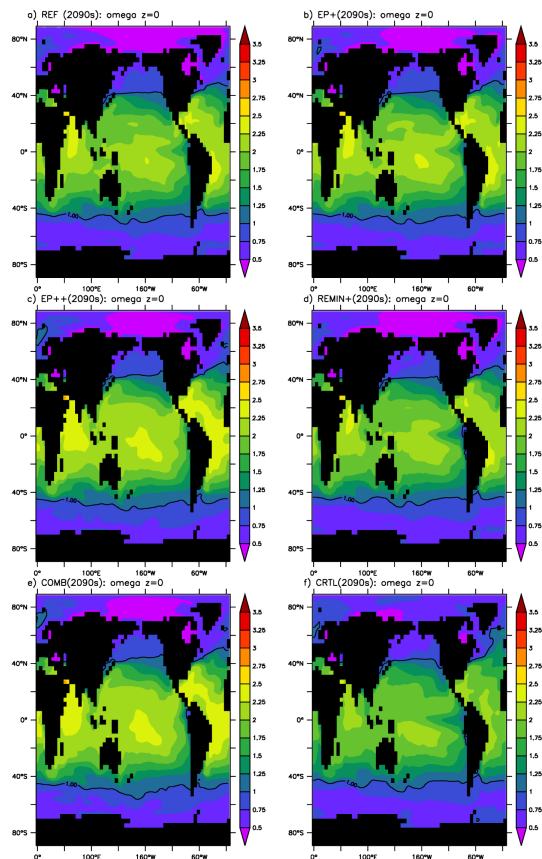
Fig. 5. Annual mean surface aragonite saturation state during the 2090–2100 period for **(a)** REF; **(b)** EP+ ; **(c)** EP++; **(d)** REMIN+; **(e)** COMB and **(f)** CTRL simulations.
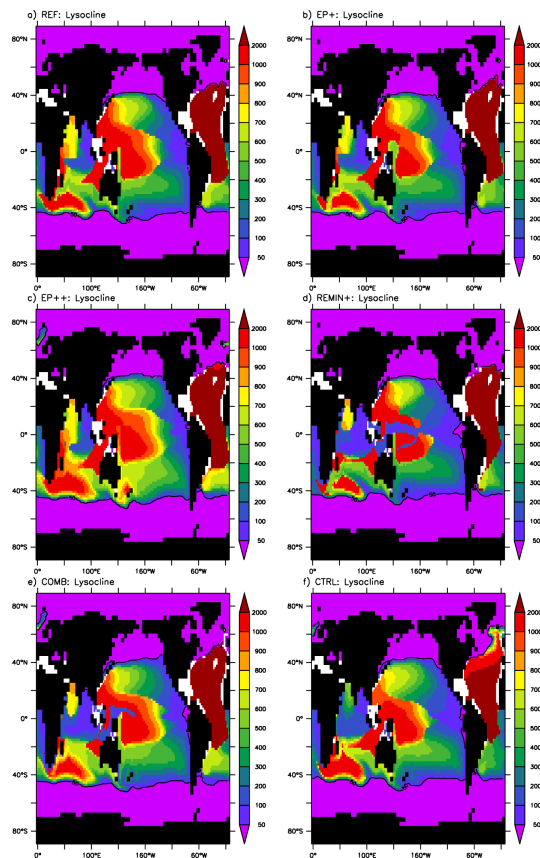
Fig. 6. Annual mean depth of the aragonite lysocline (m) during the 2090–2100 period for: **(a)** REF; **(b)** EP+ ; **(c)** EP++; **(d)** REMIN+; **(e)** COMB and **(f)** CTRL simulations.
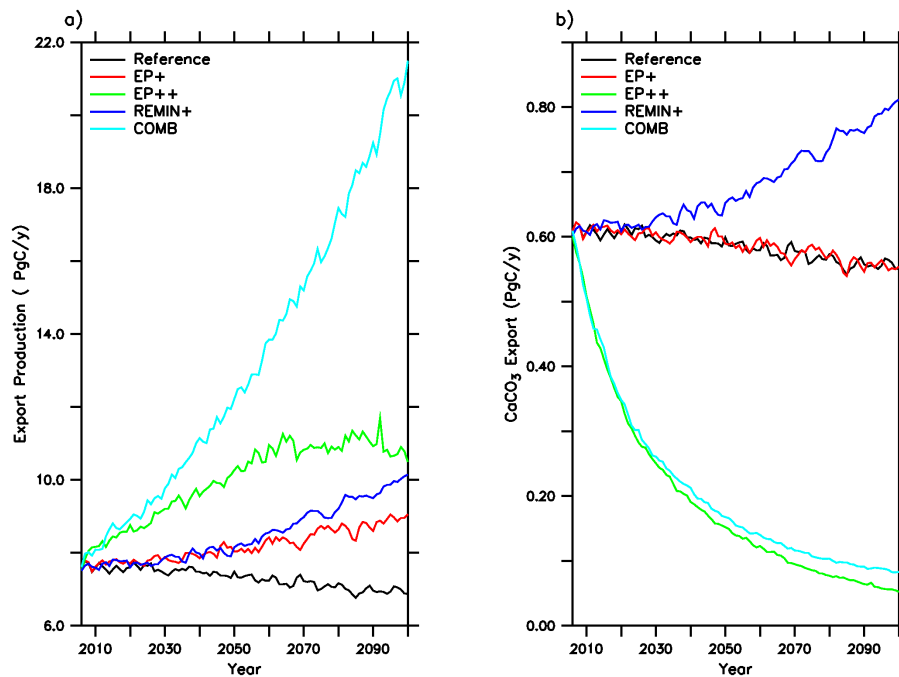
Fig. 7. (a) Projected global export of POC from the upper 100 m of the ocean. **(b)** Projected global export of PIC from the upper 100 m of the ocean.
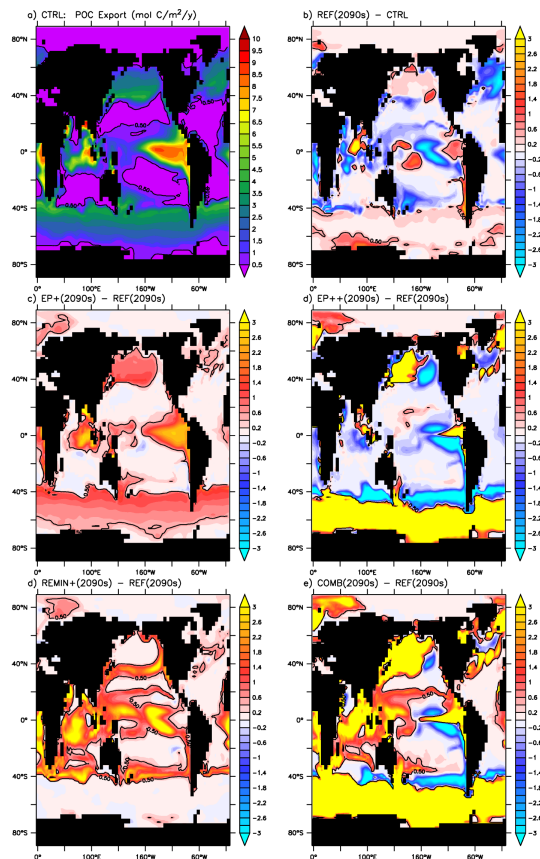
Fig. 8. Export production ($\mathrm{mol\,C\,m^{-2}\,y^{-1}}$) from the **(a)** CTRL in 1850; **(b)** the change in 2090–99 period for REF relative to **(a)**. For the 2090–99 period the change relative to REF for **(c)** EP+; **(d)** EP++; **(e)** REMIN+; **(f)** COMB simulations.
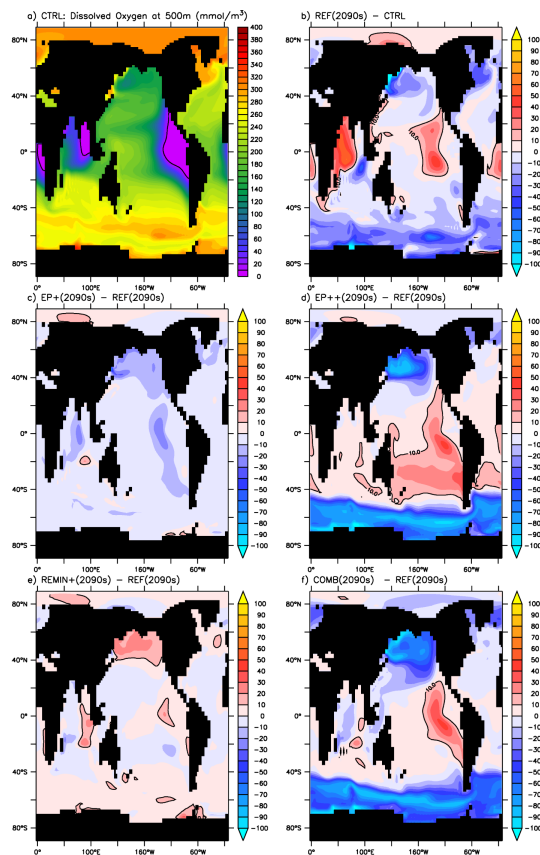
Fig. 9. Dissolved oxygen ($\mu mol\,L^{-1}$) at 500 m for **(a)** CTRL in 1850 and the difference relative to **(a)** in the 2090–99 period for **(b)** REF. For the 2090–99 period the change relative to REF for **(c)** EP+; **(d)** EP++; **(e)** REMIN+; **(f)** COMB simulations.
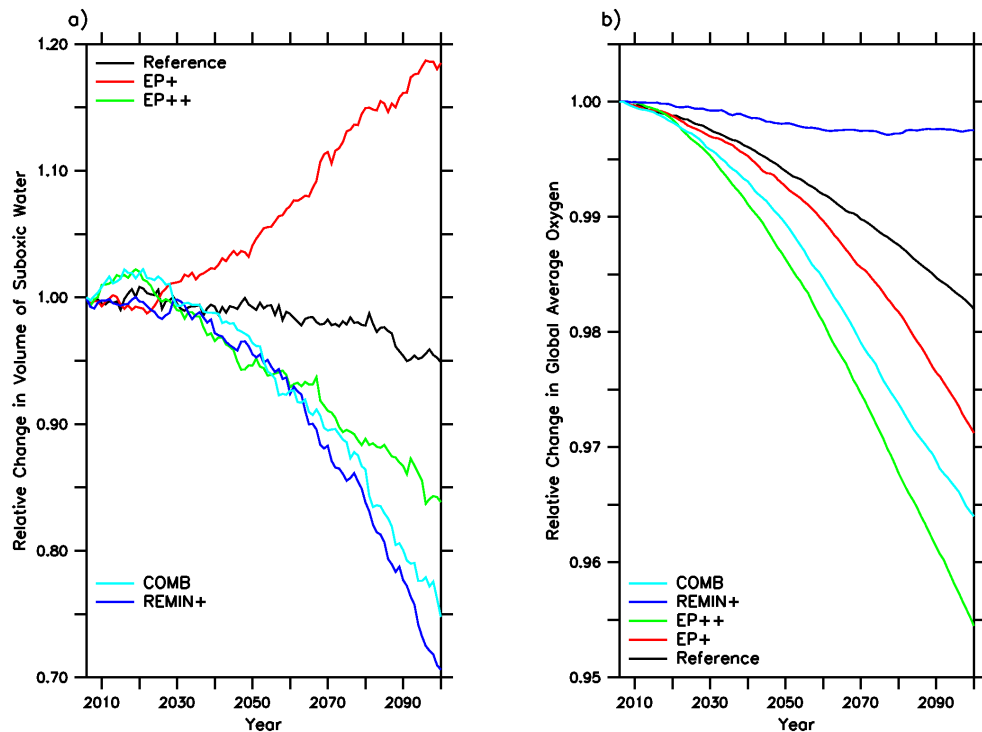
Fig. 10. **(a)** Simulated change in the volume of suboxic water relative to the simulated present-day (2006) value. **(b)** Simulated change in the global ocean inventory of dissolved oxygen relative to the simulated 2006 value.